Drying *Tectona grandis* Boards Using the Simulating Solar Kiln Conditions Technique

Khamtan Phonetip,[a,*] Graham Ian Brodie,[b] Douangta Bouaphavong,[a] Latsamy Boupha,[a] and Somxay Khambouddaphan [a]

Timber cracking, drying stress residuals, and the change of moisture content profile were investigated during the drying of *Tectona grandis* boards in a conventional laboratory kiln. The study applied a technique that simulated solar kiln conditions using a conventional laboratory kiln to dry timber, based on Vientiane's climatic conditions (Laos). The theoretical recharge and discharge model was used to generate the potential drying schedule for the Vientiane area; then the drying schedule was mimicked in a conventional laboratory kiln. Timber cracking and drying stress residual were monitored and measured using Image J software, and the change of moisture content profile was determined, based on the oven dry method. Measured moisture content data were compared with the theoretical drying model. The results showed that teak boards, of 25 mm thick, had no cracking. The drying stress residual was 0.8 ± 0.3 mm with the maximum of 1.53 mm. The initial average moisture content of 62% decreased to 12% within 16 d, while the case and core moisture contents reached 12% and 14%, respectively. The drying model described the changes of moisture content profile during drying, with a maximal error of 5%.

Keywords: Tectona grandis; Drying timber; Simulating solar kiln conditions; Solar drying schedule

*Contact information: a: Department of Forest Economics and Wood Technology, Faculty of Forest Sciences, National University of Laos, Dongdok Campus, Xaythany District, Vientiane Capital, Lao PDR; b: Faculty of Veterinary and Agricultural Sciences, Dookie Campus, The University of Melbourne, Nalinga Rd. Dookie, VIC 3647, Australia; *Corresponding author: khamtanfof@gmail.com*

INTRODUCTION

Drying of timber is the most important part of wood processing before it is processed for furniture or wood productions. There are several drying methods that have been applied to drying timber. For instance, steam kilns, microwave, vacuum driers, dehumidifiers, and solar kilns, *etc.*, have all been used.

Simulation has also been widely used in many fields (Fortin *et al.* 2004; Hossain *et al.* 2005; Roza 2005; Shenga *et al.* 2015) to better understand processes or mimic other systems. A numerical simulation for predicting drying rate and temperature inside a solar kiln has been developed by Hasan and Langrish (2014). Physical simulation is also possible, as suggested by Roza (2005). Thus, Phonetip *et al.* (2018a) trialed and found that the physical simulation of solar kiln conditions, using a conventional kiln, was possible.

Laos is one of the countries that is located in tropical latitudes, where the solar radiation is high (Simpson and Tschernitz 1984). It was also confirmed that solar kiln drying can be suitable for Laos (Phonetip *et al.* 2018b). However, drying timber, using solar kiln in Laos, is not yet available, due to the limitation of technical assistance. Only conventional kilns have been used in wood industry in Laos. Therefore, Phonetip *et al.* (2018a) introduced simulating solar kiln conditions, using a conventional kiln, for

conducting experiments in drying timber. The authors found that the accuracy was ± 2 °C compared with the actual oscillation of temperature inside the solar kiln. Mimicking temperatures can be derived from Phonetip *et al.* (2017c); however, Brodie (2005) and Spencer (1971) also developed a predictive model for temperature inside a solar kiln.

One of the important drying quality components is the moisture content profile across the thickness of the boards, which could contribute to timber cracking, due to high variation of moisture content in the boards (Phonetip *et al.* 2018c). A method of predicting moisture content profile, in the cross-section of boards, has been developed (Phonetip *et al.* 2018a).

Luang Prabang Province in Laos has 15,000 ha of teak. This is one of the timber species that is being increased in plantation area and distributed to the wood processing sector in Laos. Teak has been promoted for domestic wood processing, with the aim of mobilizing this teak resource as an alternative to timber from natural forests (Smith *et al.* 2017). The total areas of teak plantation in Lao PDR was estimated to be approximately 40,000 ha (Midgley *et al.* 2017). Therefore, understanding of drying of this timber species could contribute to improving drying quality and provide insights into parameters such as drying time and timber quality after drying. The period from February until June offers high solar radiation in Laos (Simpson and Tschernitz 1984; Surface Meteorology and Solar Energy (SSE) 2014; Selective Asia Ltd. 2017; Sun Path Chart Program 2019). Additionally, Phonetip *et al.* (2018b) found that the Faculty of Forestry Sciences (Vientiane Capital City, Laos) is one of the most suitable locations for drying timber using solar kilns.

This study aimed to investigate timber cracking, drying stress residual, and the change of moisture content profile during the drying process in a conventional laboratory kiln, which was programmed to simulate solar kiln conditions.

EXPERIMENTAL

Materials

Three teak wood board specimens derived from Napo village, Sangthong district, Vientiane Capital City, Laos, were used in this study. These boards were stacked into a larger timber charge in the kiln, being placed at the bottom, middle, and top of a stack of boards, with spacers of 25 mm × 25 mm between the boards. The full capacity of the conventional laboratory kiln (CAXE Environmental and Thermal Engineering, Binh Duoang, Vietnam) was 2 m^3. Capturing images for the specimens (cross-cut section) was done by scanning images with 1200 dpi resolution using EPSON L360 scanner (Model: C462H; Epson Philippines Corp, Ortigas Center Pasig City 1605, Philippines). All images were analyzed using Image J software (Version 1.49v, National Institutes of Health, Bethesda, MD, USA) for measuring the internal check.

Methods

Drying schedule

The temperature model, for predicting temperature inside a solar kiln, derived from Brodie (2005) and Phonetip *et al.* (2017a), was used to generate the daily pattern of temperature variation characteristic of a drying kiln being used in Vientiane, Laos, as a cycle over 24 h. The oscillation of temperature is plotted in Fig. 1.

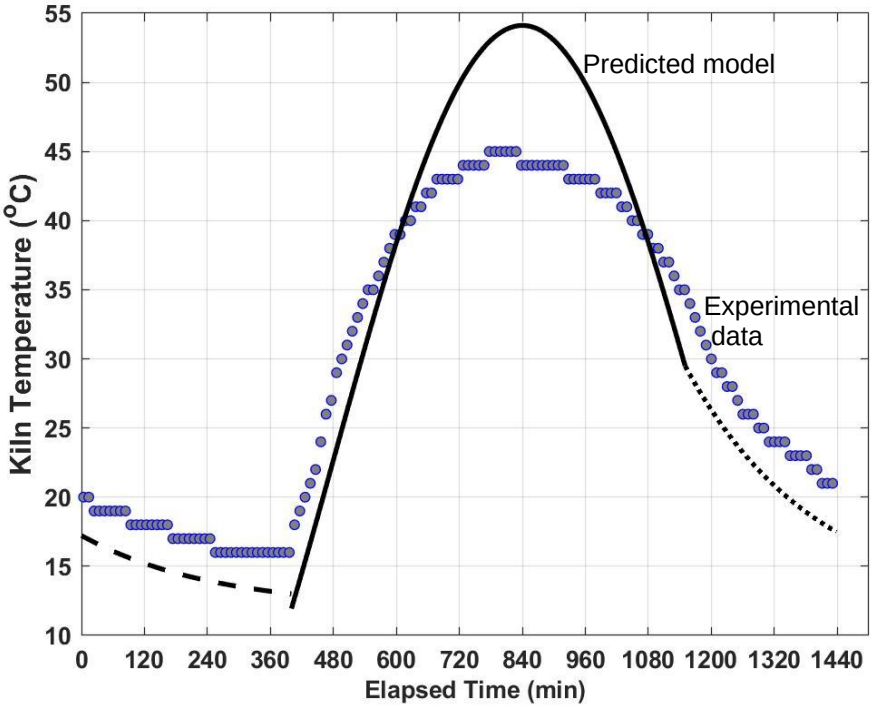

Fig. 1. Predicted temperature derived from recharge and discharge model by Brodie (2005)

The authors noted that the maximum level of predicted temperature was 54 ℃ in April, so to decrease moisture content (MC) in boards, decreasing relative humidity (RH) was considered. This was generated, as shown in Fig. 2.

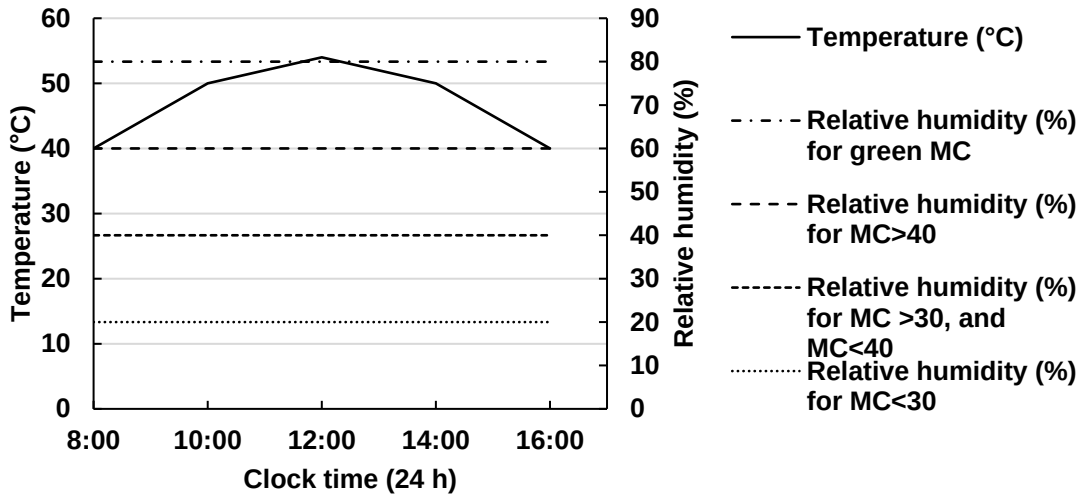

Fig. 2. Drying schedule derived from previous suggestions (Brodie 2005; Phonetip *et al.* 2017a, 2018a)

Modelling the drying dynamics

Several factors affect wood drying rates, but the drying occurs when the MC of harvested wood is above the equilibrium moisture content (EMC). According to Simpson (1998), EMC is dependent on RH and temperature (T) such that,

$$EMC = \frac{1800}{W}\left(\frac{Kh}{1-Kh} + \frac{K_1Kh+2K_1K_2K^2h^2}{1+K_1Kh+K_1K_2K^2h^2}\right) \quad (1)$$

where

$$W = 349 + 1.29\,T + 0.0135\,T^2 \quad (2)$$

$$K = 0.805 + 0.000736\,T + 0.00000273\,T^2 \quad (3)$$

$$K_1 = 6.27 - 0.00938\,T - 0.000303\,T^2 \quad (4)$$

$$K_2 = 1.91 + 0.0407\,T - 0.000293\,T^2 \quad (5)$$

$$h = \frac{RH}{100} \quad (6)$$

Timber drying is described using Fick's second law, in one spatial dimension, as follows,

$$\frac{\partial M}{\partial t} = D\,\frac{\partial^2 M}{\partial x^2} \quad (7)$$

where t is time (s), x is spatial dimension (m), D is diffusion coefficient ($m^2 \cdot s^{-1}$), and M is moisture content of the wood on a dry mass basis (%).

The general solution for the moisture diffusion equation has been provided by Crank (1979),

$$\frac{M-EMC}{M_i-EMC} = \sum_{n=1}^{\infty} \frac{2L\cos\left(\frac{\beta_n x}{l}\right)e^{-\left(\frac{\beta_n^2 Dt}{l^2}\right)}}{\left(\beta_n^2+L^2+L\right)\cos(\beta_n)} \quad (8)$$

where x is the distance from the centre of the board (m), βn is surface drying coefficient ($kg \cdot m^{-2}s^{-1}$), counted as the positive roots of β tan β is L [roots of β tan β are provided for several values of L in Carslaw and Jaeger (1959), $L = l\alpha/D$ is a dimensionless parameter, where l is half thickness of the board (m); α is evaporation rate ($m \cdot s^{-1}$); t is time (s); and D is diffusion coefficient ($m^2 \cdot s^{-1}$).

Equation 8 indicates that the outer case of wood will have a lower *EMC* than the inner core. It is also apparent that average moisture content exhibited an exponential decline with time. The average drying response for the whole board can be described by integrating Eq. 9 over the cross section of the board, yielding the general relationship:

$$\frac{M-EMC}{M_i-EMC} = Ae^{-\left(\frac{\beta_n^2 Dt}{l^2}\right)} \quad (9)$$

In this experiment, the MC was also changing with time. These changes included diurnal changes due to temperature changes through the day (Fig. 3) and the longitudinal changes according to the changes in RH as the timber reached critical values of MC (Fig. 4).

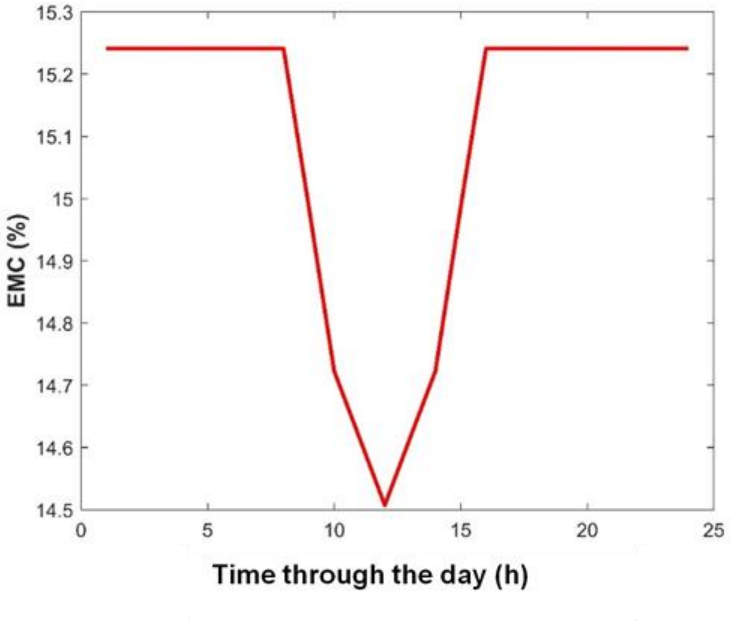

Fig. 3. Diurnal EMC change at the start of drying when the RH is 80%

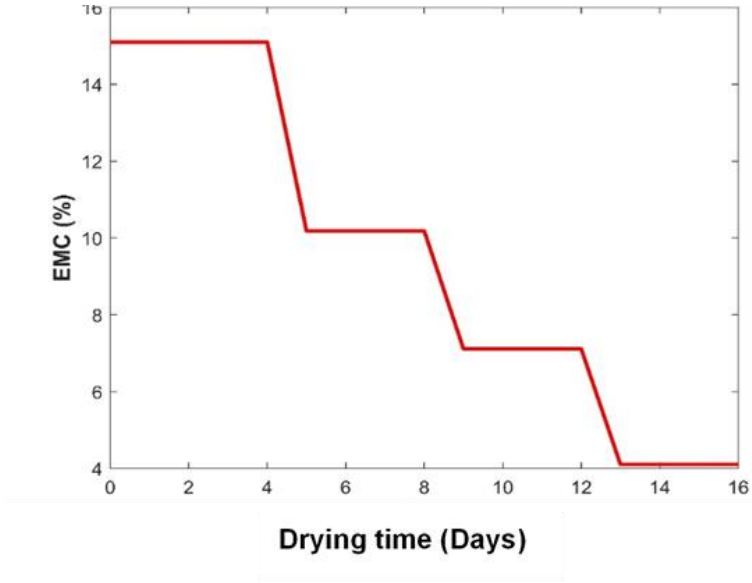

Fig. 4. Longitudinal changes in EMC during the drying process

The results of predicted MCs were then validated with actual MCs, derived from experimental outcomes. Specimens were taken from the three sample boards, as per Fig. 5, every day at 4 pm.

Measurement of internal checking was in accordance with Phonetip *et al.* (2017b), and the MC profile measurement techniques were derived from Phonetip *et al.* (2018a). However, a modification was made. For instance, taking specimen for the MC profile was done by sawing the boards, not drilling, because of the high variation of MC that was caused by the drilling process in the previous study.

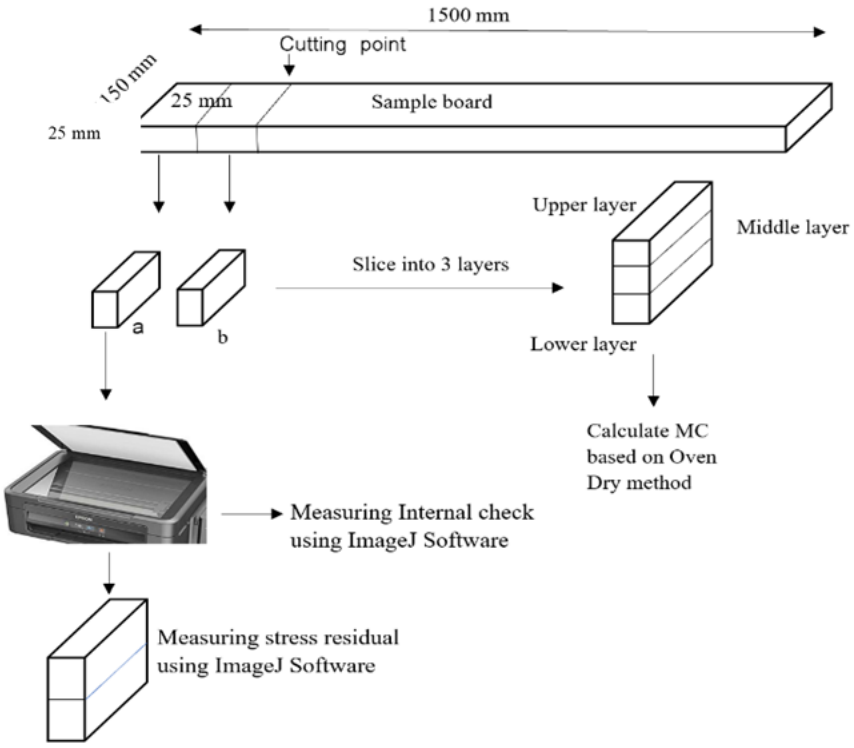

Fig. 5. Process of preparing specimen for MC profiles on b, and the internal check and stress residual on a

RESULTS AND DISCUSSION

Drying conditions inside the conventional laboratory kiln showed that oscillation of temperature coincided with the set temperatures during the simulation period at clock times of 10.00, 12.00, 14.00, 16.00, and 18.00 h through the day (Fig. 6). The absolute differences in temperature between the simulated temperatures at each clock time was ± 4 °C, ± 4 °C, ± 2 °C, ± 1 °C, and ± 2 °C, respectively. At the first stage of drying, the absolute difference in temperature was similar (2 °C) to that finding by Phonetip *et al.* (2018a). The relative humidity fluctuated from the set point of RH = 80% (81 ± 12%) during the first stage of drying (Fig. 6 (a)). The RH was 65 ± 15% (Fig. 6(b)) when it was set at 60%; the RH was 48 ± 12% (Fig. 6(c)) when set to 40%; and the RH was 30 ± 9% (Fig. 6(d)) when set to 20%. The variation of relative humidity was between ± 12% to ± 15% from the set point of RH for 80%, 60%, and 40% but the required set point for 20% of RH could be reached within a short time, *i.e.*, the RH reached 20% at 15.00 to 16.00 (Fig. 6(d)). It was also apparent that the relative humidity increased in the middle of the simulated day when the temperature approached a maximum. The results reflect the fact that specimens were taken for checking the stress residual and MC at 4 pm every day (door opened), as stated in the Methods section. During this time the kiln conditions were interrupted, which resulted in increased relative humidity. In addition, the output may be affected by the kiln capacity.

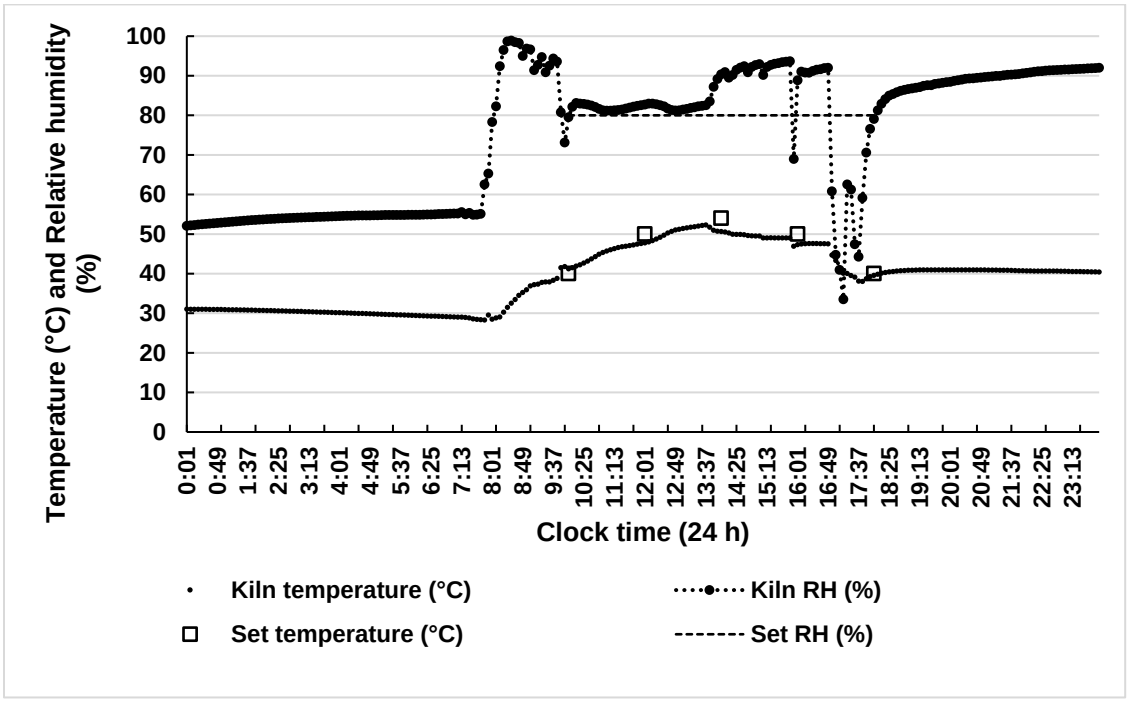
Temperature (°C) and Relative humidity (%)
100
90
80
70
60
50
40
30
20
10
0
0:01
0:49
1:37
2:25
3:13
4:01
4:49
5:37
6:25
7:13
8:01
8:49
9:37
10:25
11:13
12:01
12:49
13:37
14:25
15:13
16:01
16:49
17:37
18:25
19:13
20:01
20:49
21:37
22:25
23:13
Clock time (24 h)
Kiln temperature (°C)
Kiln RH (%)
Set temperature (°C)
Set RH (%)

(a)

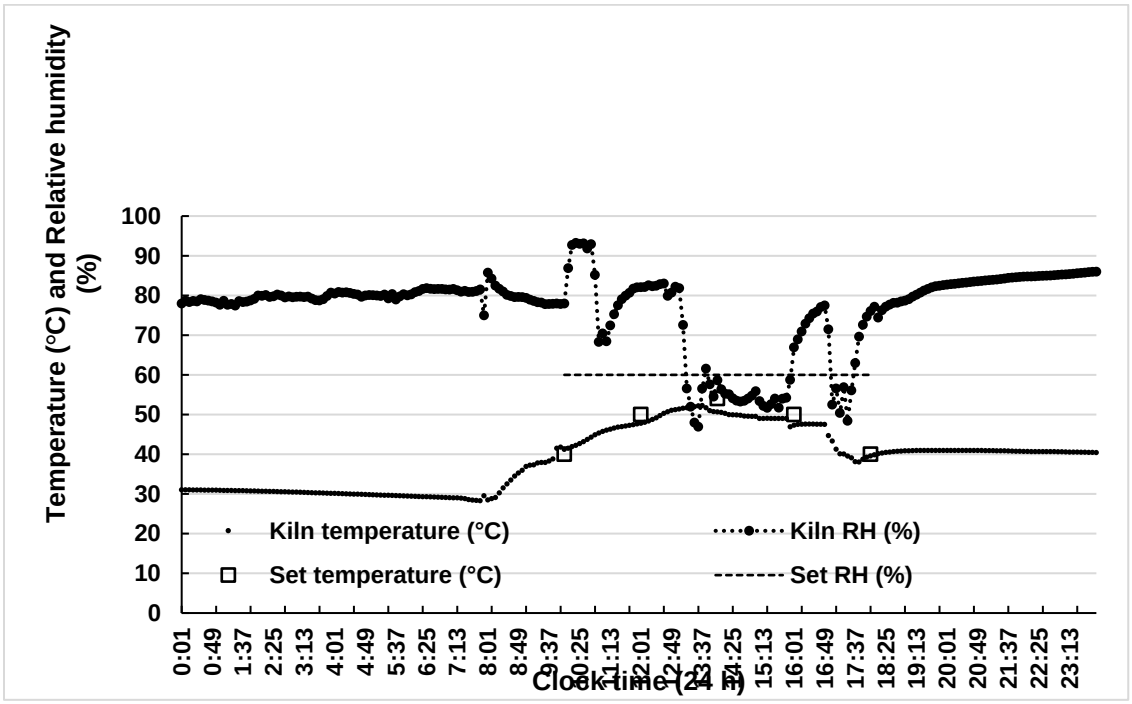
Temperature (°C) and Relative humidity (%)
100
90
80
70
60
50
40
30
20
10
0
0:01
0:49
1:37
2:25
3:13
4:01
4:49
5:37
6:25
7:13
8:01
8:49
9:37
10:25
11:13
12:01
12:49
13:37
14:25
15:13
16:01
16:49
17:37
18:25
19:13
20:01
20:49
21:37
22:25
23:13
Clock time (24 h)
Kiln temperature (°C)
Kiln RH (%)
Set temperature (°C)
Set RH (%)

(b)

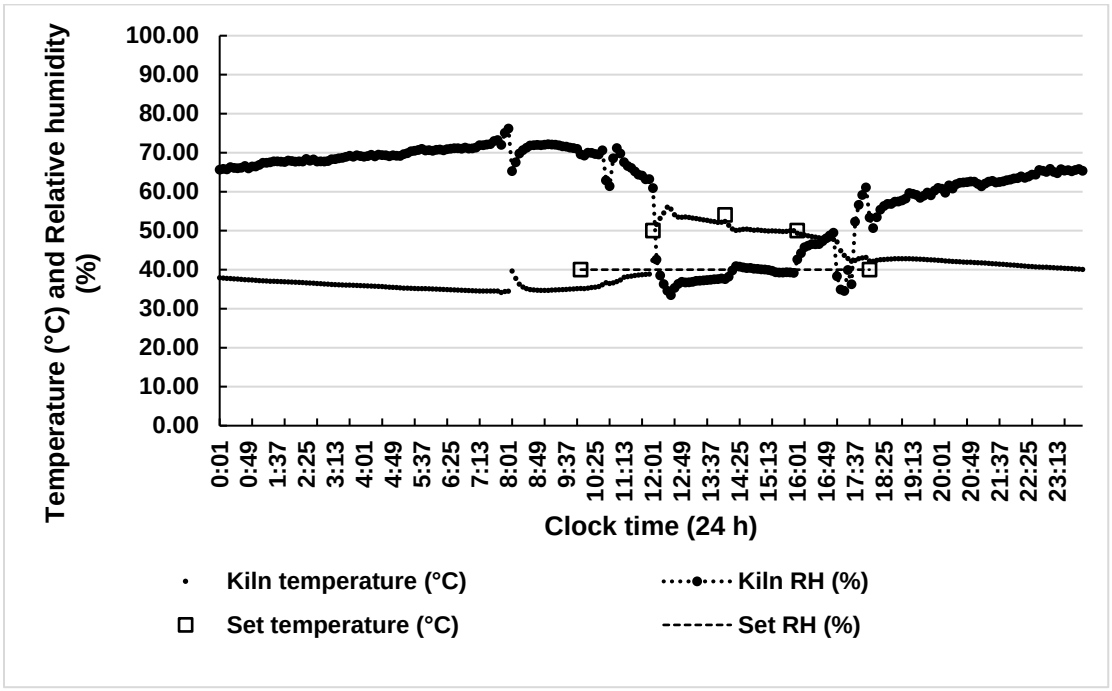

(c)

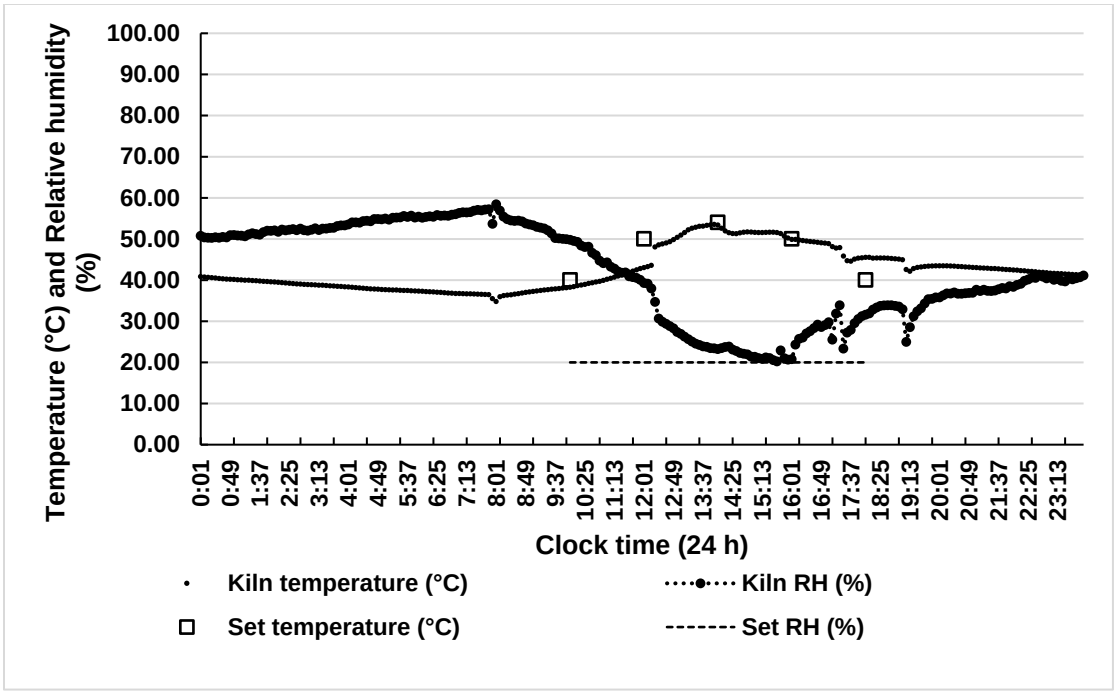

(d)

Fig. 6. Kiln condition at RH of 80% (a), 60% (b), 40% (c), and 20% (d)

The Change of Moisture Content Profile

Figure 7(a) shows both the modelled and measured decrease in mean moisture content over time. The predicted EMC, and the measured MC for the top case, bottom case, and core of a sample board were included. The MC profile, across the board, as a function of drying time, is shown in Fig. 7(b).

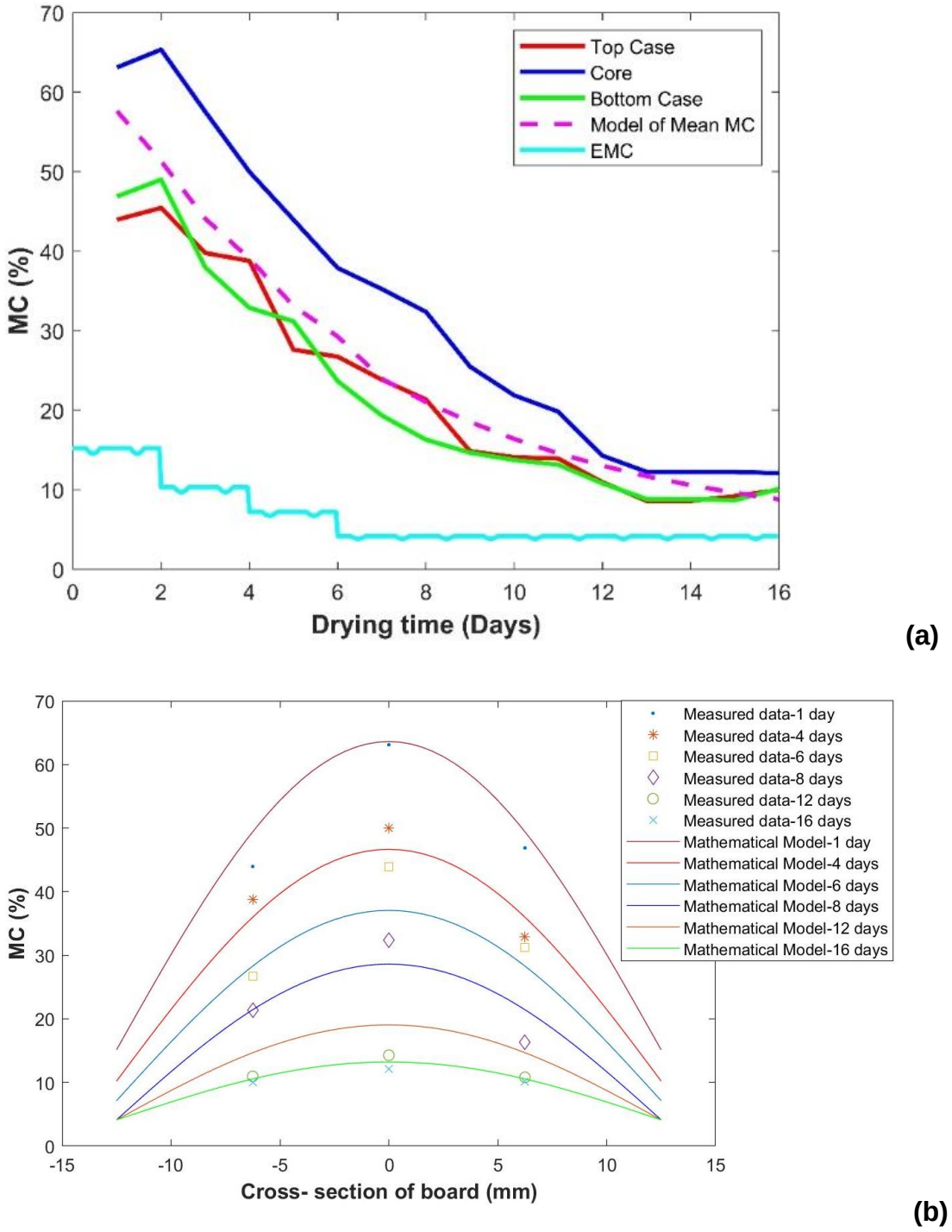

Fig. 7. (a): Drying profile showing the EMC changes; (b): the drying model described by Eq. 9 and drying model for MC content profile

The initial mean moisture content changed from 62% down to 12% over 16 d. Drying rate was considered as a function of each EMC condition, which was derived from the drying schedule (Fig. 2). For instance, EMC at the first stage of drying was 15% for day 1 to day 2 (2 d). The second stage EMC was 10% for 2 days from day 2 to day 4. The third stage EMC was 8% for day 4 to day 6, and the last stage had an EMC of 5% from day

6 to day 16 (10 d). The drying rate for EMC = 15% decreased 6%/day, at EMC = 10% the drying rate was 5%/day, at EMC = 8% the drying rate was 5%/day, and EMC = 5% the drying rate was 2.2%/day.

The mathematical models for drying, presented in Eqs. 8 and 9, were implemented as functions in MatLab (The MathWorks, Inc., Version 2020a, Natick, MA, USA). They describe the moisture content profile across the cross-section of the board (Eq. 8) and the mean MC of the board (Eq. 9) against drying time. The experimental data were plotted, along with the model's predictions, to validate the modelling. The absolute error between the measured MC and that predicted by the mathematical modelling, for the core MC on days 1, 4, 6, 8, 12, and 16, was 1%, 3%, 6%, 3%, 4%, and 1%, respectively. For the top and bottom cases, the absolute errors in MC were 4%, 1%, 0%, 3%, 5%, and 0%, respectively. These errors were due to inaccuracies within the chosen parameters in the model and some variability in the conditions in the kiln. Overall, the model adequately predicted the MC in the test boards and could be used to forecast the expected drying performance of the kiln system and potentially optimize the design of future experiments and kiln systems.

Internal checks in the board were monitored and assessed using the Image J software, as explained in the methods section. The results showed that no internal checking was found in boards during drying (Fig. 8). This may indicate that the boards were stress free and the moisture content gradient was minimal. The mean maximum drying stress residual was 1.5 ± 0.2 mm, where the RH was changed from 40% to 20% (day 7). At the end of the drying (day 16), the mean drying stress residual was 0.3 mm (Fig. 9(a)). This could imply that the oscillation of the temperature between 30 ℃ and 54 ℃ with the variation in RH according to the imposed drying schedule (*i.e.*, RH = 80%, 60%, 40%, and 20% (Fig. 6)) did not cause internal checking in the teak boards.

The ramping of initial temperature from 30 ℃ to 54 ℃ with RH = 80%, were according to the kiln schedule coded as "245(T10-D4S)", as recommended by Boone *et al.* (1988). In addition, moisture content gradient was also one of the drying parameters to indicate the risk of internal checking in boards. In 40-mm-thick *Eucalyptus delegatensis*, dried in oscillation conditions of temperature (20 ℃ to 45 ℃) with RH between 60% and 80% (Phonetip *et al.* 2018e), internal checks occurred at an MC gradient of between 30% and 40%. However, the MC gradient of 34% in the teak boards did not cause any internal checks under the oscillation conditions of the second stage of drying, as shown in Fig. 6(b), with highest temperature of 54 ℃.

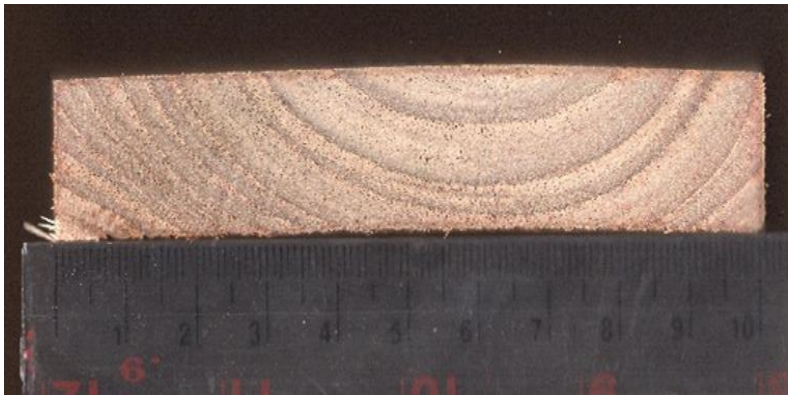

Fig. 8. Crosscut for observing the internal check

Drying stress residual was monitored and measured every day. The values of the stresses, from day 1 until day 16, are shown in Fig. 9(a). Under the drying schedule (Fig. 2), the drying stress residual fluctuated. The maximum stress for the first stage was 0.76 mm (day 1), in the second stage it was 0.91 mm (day 4), in the third stage it was 1.19 mm (day 6), and in the last stage, from day 7 to day 16, when the RH was set at 20%, the maximum drying stress residual reached 1.53 mm on day 7. However, the lowest value was found on day 15 (0.3 mm). Each stage of drying created some drying stress residual. The values were plotted against moisture content gradient (Fig. 9(b)); however, there was no correlation between these two factors (R^2 = 0.046) based on these particular drying conditions (Fig. 2). This could imply that the increase of moisture content gradient did not influence drying stress residual during drying, as stated by Phonetip *et al.* (2018c).

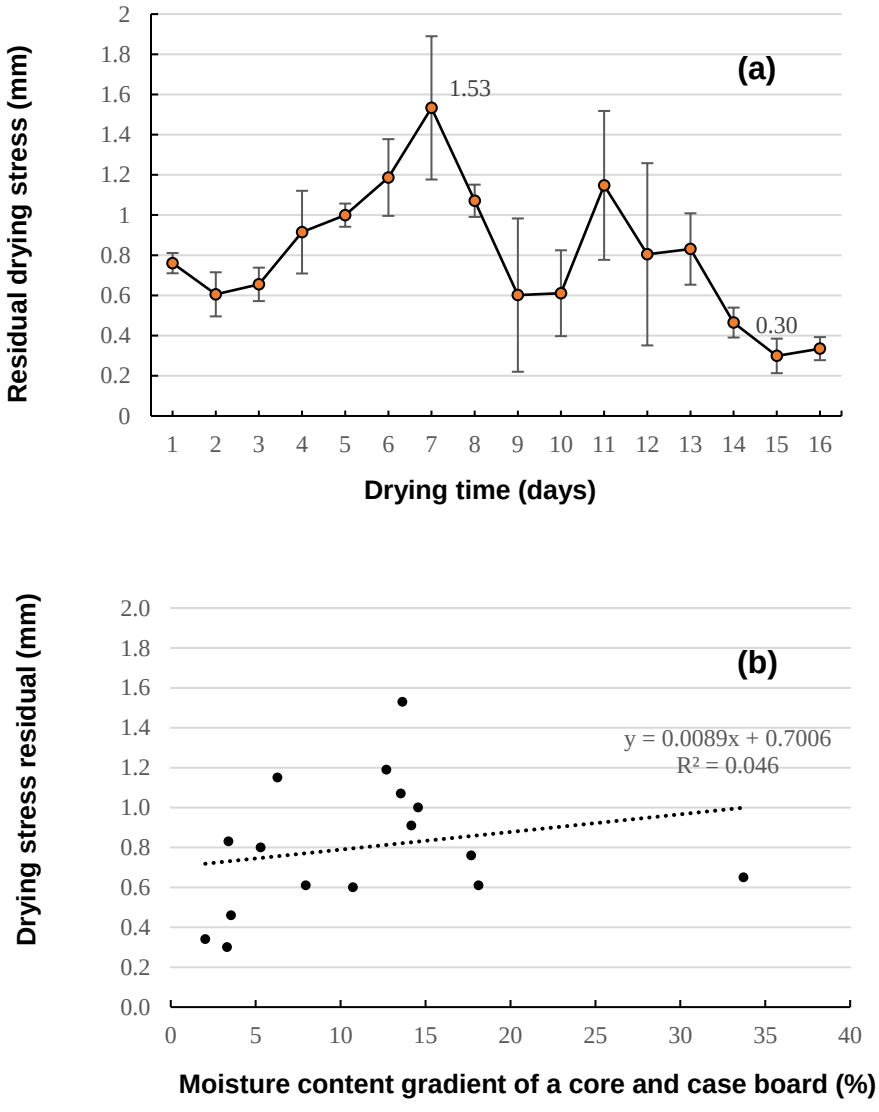

Fig. 9. Residual drying stress during drying process (a), and the correlation between the drying stress residual and moisture content gradient (b)

CONCLUSIONS

1. The drying of *Tectona grandis* boards using the simulated solar kiln conditions took 16 d from the initial moisture content of 62% to 12%, under oscillating drying conditions.
2. The predicting model described moisture content profile during drying. The model calculated the drying rate, as per drying conditions, with an accuracy of 5% variation from the measured moisture content.
3. There were no internal checks found during the entire drying experiment with the maximum moisture content gradient of 34% and the maximum of drying stress residual of 1.53 mm.

REFERENCES CITED

Boone, S. R., Kozlik, C. J., Bois, P. J., and Wengert, E. M. (1988). *Dry Kiln Schedules for Commercial Woods* (General Technical Report FPL-GTR-57), U. S. Department of AgricuIture, Forest Products Laboratory, Maddison, WI, USA.

Brodie, G. (2005). *Microwave Timber Heating and Its Application to Solar Drying*, Ph.D. Dissertation, Institute of Land and Food Resources, the University of Melbourne, Melbourne, Australia.

Carslaw, H. S., and Jaeger, J. C. (1959). *Conduction of Heat in Solids*, Clarendon Press, Oxford, England.

Crank, J. (1979). *The Mathematics of Diffusion*, J. W. Arrowsmith Ltd., Bristol, England.

Fortin, Y., Defo, M., Nabhani, M., Tremblay, C., and Gendron, G. (2004). "A simulation tool for the optimization of lumber drying schedules," *Drying Technology* 22(5), 963-983. DOI: 10.1081/drt-120038575

Hasan, M., and Langrish, T. (2014). "Numerical simulation of a solar kiln design for drying timber with different geographical and climatic conditions in Australia," *Drying Technology* 32(13), 1632-1639. DOI: 10.1080/07373937.2014.915556

Hossain, M. A., Woods, J. L., and Bala, B. K. (2005). "Simulation of solar drying of chilli in solar tunnel drier," *International Journal of Sustainable Energy* 24(3), 143-153. DOI: 10.1080/14786450500291859

Midgley, S. J., Stevens, P. R., and Arnold, R. J. (2017). "Hidden assets: Asia's smallholder wood resources and their contribution to supply chains of commercial wood," *Australian Forestry* 80(1), 10-25. DOI: 10.1080/00049158.2017.1280750

Phonetip, K., Brodie, G., Ozarska, B., and Belleville, B. (2017a). " Drying timber in a solar kiln using an intermittent drying schedule of conventional laboratory kiln," *Drying Technology Journal* 37(10), 1300-1312. DOI: 10.1080/07373937.2018.1496337

Phonetip, K., Ozarska, B., and Brodie, G. (2017b). "Comparing two internal check measurement methods for wood drying quality assessment," *European Journal of Wood and Wood Products* 75, 139-142. DOI: 10.1007/s00107-016-1115-1

Phonetip, K., Ozarska, B., Brodie, G., Harris, G., and Belleville, B. (2017c). "Quality assessment of the drying process for *Eucalyptus delegatensis* timber using greenhouse solar drying technology," *European Journal of Wood and Wood Products* 77, 57-62. DOI: 10.1007/s00107-018-1364-2

Phonetip, K., Brodie, G., Ozarska, B., and Belleville, B. (2018a). "Simulating solar kiln conditions using a conventional kiln," *BioResources* 13(2), 3740-3752. DOI: 10.15376/biores.13.2.3740-3752

Phonetip, K., Brodie, G., Ozarska, B., Belleville, B., and Boupha, L. (2018b). "Applying a GIS-based fuzzy method to identify suitable locations for solar kilns," *BioResources* 13(2), 2785-2799. DOI: 10.15376/biores.13.2.2785-2799

Phonetip, K., Ozarska, B., Belleville, B., and Brodie, G. I. (2018c). "Comparing two intermittent drying schedules for timber drying quality," *Drying Technology* 37(2), 186-197. DOI: 10.1080/07373937.2018.1445638

Roza, Z. C. (2005). *Simulation Fidelity Theory and Practice: A Unified Approach to Defining, Specifying and Measuring the Realism of Simulations*, Delft University Press, Delft, Netherlands.

Selective Asia Ltd. (2017). "Laos' weather," (https://www.selectiveasia.com/laos-holidays/weather), Accessed 17 Oct 2017.

Shenga, A. P., Bomark, P., Broman, O., and Sandberg, D. (2015). "Simulation of tropical hardwood processing-sawing methods, log positioning, and outer shape," *BioResources* 10(4), 7640-7652. DOI: 10.15376/biores.10.4.7640-7652

Simpson, W., and Tschernitz, J. (1984). "Solar dry kiln for tropical latitudes," *Forest Products Journal* 34(5), 25-34.

Simpson, W. T. (1998). *Equilibrium Moisture Content of Wood in Outdoor Locations in the United States and Worldwide* (RN-0268), United States Department of Agriculture, Washington, DC, USA. Technical report.

Smith, H. F., Ling, S., and Boer, K. (2017). "Teak plantation smallholders in Lao PDR: What influences compliance with plantation regulations?," *Australian Forestry* 80(3), 178-187. DOI: 10.1080/00049158.2017.1321520

Spencer, J. W. (1971). "Fourier series representation of the position of the sun," *Search* 2, 162-172.

Surface Meteorology and Solar Energy (2014). "NASA surface meteorology and solar energy tables," (https://eosweb.larc.nasa.gov), Accessed 12 Aug 2014.

Sun Path Chart Program (2019). "Solar radiation monitoring laboratory, University of Oregon," (http://solardat.uoregon.edu/SunChartProgram.php), Accessed 5 April 2020.

Article submitted: August 5, 2020; Peer review completed: October 10, 2020; Revised version received and accepted: October 11, 2020; Published: October 15, 2020.
DOI: 10.15376/biores.15.4.9075-9087